Available online at www.sciencedirect.com
SCIENCE DIRECT®
Journal of Sound and Vibration 268 (2003) 15–31
JOURNAL OF SOUND AND VIBRATION
www.elsevier.com/locate/jsvi

Dynamic analysis of an optical fiber coupler in telecommunications

Gong Cheng, Jean W. Zu*

Department of Mechanical & Industrial Engineering, University of Toronto, 5 King's College Road, Toronto, Ont., Canada, M5S 3G8

Received 22 October 2001; accepted 4 November 2002

Abstract

This paper studies the vibration of an optical fiber coupler which is used in telecommunications subjected to a half sine shock. The emphasis is focused on analyzing the vibration response of the optical fibers inside the coupler and examining the influence of various coupler parameters on the vibration of the optical fibers, since their dynamic behavior is a critical factor in optical fiber communications. A simplified model of the optical fiber coupler is proposed, which consists of a beam and a string representing the substrate and the bundle of the optical fibers of the coupler, respectively. The beam and the string are bonded at four points using adhesive material, and therefore the boundary conditions for their equations of motion are coupled, which increases the complexity of the problem. For the string, two models are developed— the linear model assumes that the tension in the string is constant, while the non-linear one takes into account large transverse deflection and tension variation. With each model, both analytical study and numerical simulations for the vibration of the system under a half shock are carried out. Furthermore, numerical results are compared between the two models. Finally, parametric study leads to conclusions which are of practical importance to the design of optical fiber couplers.

1. Introduction

The term "optical fiber coupler" began to appear in many optics and telecommunications papers, e.g., Refs. [1–3], after the late 1970s when the glass fiber with adequate performance was developed. It refers to a basic interconnection element for assembling a variety of distribution networks that employ optical fibers. Its function is to demultiplex or multiplex optical signals from one fiber or optical signal path to more fibers or signal paths. For a majority of

*Corresponding author. Tel.: +1-416-978-0961; fax.: +1-416-978-7753.
E-mail address: zu@mie.utoronto.ca (J.W. Zu).

0022-460X/03/$ - see front matter
doi:10.1016/S0022-460X(02)01575-4

communication networks, the performance of the coupling elements rather than the transmission characteristics of the fiber lines themselves limits the performance of the networks and determines the optimum network configuration. Therefore, optical fiber couplers play a very important role in optical fiber communications.

A typical optical fiber coupler is composed of a bundle of fused optical fibers, a substrate, and a steel tube. The bundle of optical fibers is bonded to the substrate at several points using adhesive material, as shown in Fig. 1. The substrate provides the housing for the optical fibers. The substrate and the fibers are wrapped inside the steel tube. In addition, rubber pads are placed between the steel tube and the substrate at each end of the coupler to cushion the impact on communication lines.

Under shocks and impacts on communication lines, optical fibers in couplers may experience large vibrations and occasional breaks, which severely interfere with proper signal transmission. For example, the coupler may exhibit excess insertion loss, potential modal distortion, dispersion and bandwidth-limiting effects. A major reason for the problem is the lack of proper design of the coupler to satisfy its required dynamic characteristics. Vibration analysis is essential to understanding the dynamic characteristics of a coupler. Moreover, the mechanical component of couplers presently available on the market is designed mainly based on experience and on trial and error. Hence, the vibration analysis of an optical fiber coupler has become imperative.

Since the 1980s, optical fiber couplers have been attracting the attention of many researchers. Most of their work is, however, concentrated on the material structures, optical characteristics and the manufacturing methods of the couplers. No research has hitherto been found on the vibration analysis of the coupler, to the authors' knowledge. It is, therefore, the objective of this paper to investigate the vibration of the optical fiber coupler.

In the present paper, an analysis model of an optical fiber coupler is introduced, with the substrate modeled as a beam supported at each end by a spring representing the rubber pads and the optical fibers as a string, as shown in Fig. 2. The beam and the string are connected at four points representing four adhesive bonding points, and the problem thereby turns into a coupled beam-string vibration problem differing from other string or beam vibration problems which have been extensively studied [4–11]. Two models are developed for the string—the linear model assumes that the transverse deflection of the string is small and the tension in the string is constant, while the non-linear one takes into account large transverse deflection and tension variation. The study is focused on the analysis of the vibration response of the system, especially

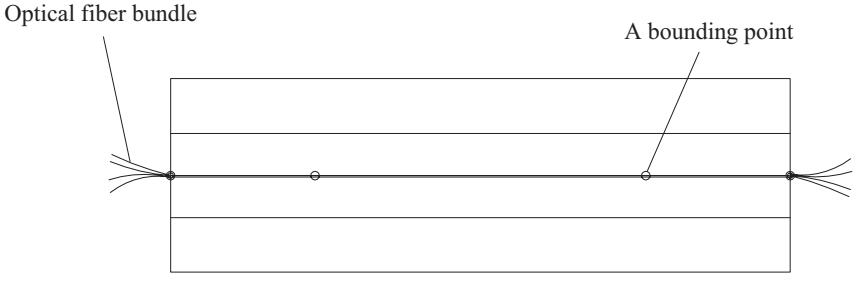

Fig. 1. Top view of a substrate.

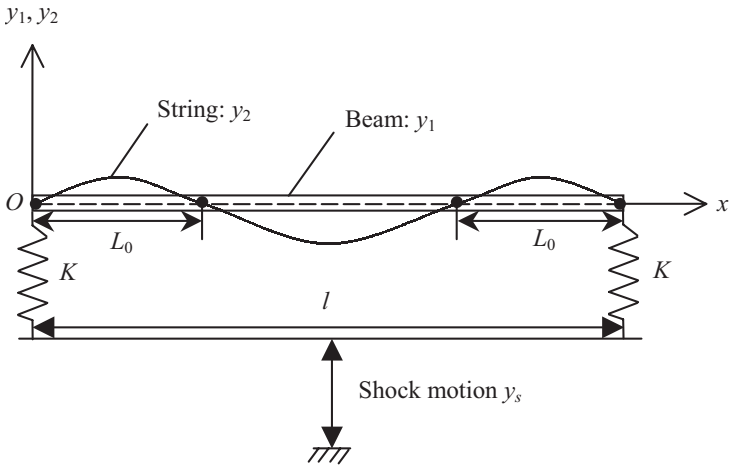

Fig. 2. A simplified model of an optical fiber coupler.

that of the optical fibers, under a half sine shock, and on the analysis of the influence of various coupler parameters upon the response of the optical fibers.

2. Dynamic analysis of the substrate

Considering the material construction and the size of the substrate and the optical fibers in a coupler, it is reasonable to model them as a beam and a string, respectively. In the following discussion, two assumptions are made: (1) the influence of the string on the vibration of the beam is neglected so that the equation of motion for the beam, together with its boundary conditions, is independent. (2) axial vibration of the beam and of the string is negligible, and only their transverse vibration is considered.

The whole system is subjected to a half sine shock motion along its length whose acceleration is in the form

$$\frac{\mathrm{d}^2 y_s(t)}{\mathrm{d}t^2} = F \sin \omega t \quad \left(0 \leqslant t \leqslant \frac{\pi}{\omega}\right), \tag{1}$$

where y_s is the displacement of the base of the system, as shown in Fig. 2, and F, ω are the amplitude and the circular frequency of the acceleration, respectively. In this study, the shock motion is assumed to be a 1000 g 0.5 ms half sine one which is commonly adopted in industry. It should also be pointed out that only the response during the shock period is considered as this is the time when the optical fiber breaks usually occur.

Let $y_1(x, t)$ be the beam deflection and $y_2(x, t)$ be the string deflection, where x is a position variable, as shown in Fig. 2. The equation of motion for the beam during $0 \leq t \leq \pi/\omega$ is derived as

$$EJ\frac{\partial^4 y_1}{\partial x^4} + \rho_1 A_1 \frac{\partial^2 y_1}{\partial t^2} = -\rho_1 A_1 F \sin \omega t, \tag{2}$$

with boundary conditions

$$\left.\frac{\partial^2 y_1}{\partial x^2}\right|_{x=0} = 0, \quad \left.\frac{\partial^2 y_1}{\partial x^2}\right|_{x=l} = 0, \quad EJ\left.\frac{\partial^3 y_1}{\partial x^3}\right|_{x=0} = -Ky_1(0,t), \quad EJ\left.\frac{\partial^3 y_1}{\partial x^3}\right|_{x=l} = Ky_1(l,t), \tag{3}$$

where E, J, ρ_1, A_1, l are Young's modulus, the moment of inertia of the cross-section, the mass density, the cross-sectional area and the length of the beam, respectively, and K denotes the spring stiffness.

The above equation of motion for the beam belongs to the classical beam problems with standard solution procedures available. The solution procedures are restated briefly below to obtain the beam response for future use in the vibration analysis of the string. Suppose the solution for the free vibration of the beam takes the form

$$\bar{y}_1(x,t) = \left(A\sin K^* x + B\cos K^* x + C\sinh K^* x + D\cosh K^* x\right)\sin(pt+\varphi), \tag{4}$$

where p is the natural frequency, φ the phase angle, A, B, C, D the unknown coefficients, and

$$K^* = \left[\frac{\rho_1 A_1}{EJ}p^2\right]^{1/4}. \tag{5}$$

The mode shapes of the beam for the boundary conditions (3) are derived as

$$Y_{1n}(x) = K_A\sin K^* x + \cos K^* x + K_C\sinh K^* x + \cosh K^* x \quad (n = 1,2,\ldots), \tag{6}$$

where

$$\begin{aligned} K_A &= \frac{\cos K^* l - \cosh K^* l + 2K\sinh K^* l/\left(EJK^{*3}\right)}{\sinh K^* l - \sin K^* l}, \\ K_C &= \frac{\cos K^* l - \cosh K^* l + 2K\sin K^* l/\left(EJK^{*3}\right)}{\sinh K^* l - \sin K^* l}. \end{aligned} \tag{7}$$

The natural frequencies p_n ($n=1, 2,\ldots$) of the beam can be obtained numerically from the equation

$$\begin{aligned} &EJK^{*3}\left(-K_A\cos K^* l + \sin K^* l + K_C\cosh K^* l + \sinh K^* l\right) \\ &- K\left(K_A\sin K^* l + \cos K^* l + K_C\sinh K^* l + \cosh K^* l\right) = 0. \end{aligned} \tag{8}$$

Assume that the solution to Eq. (2) during $0 \leqslant t \leqslant \pi/\omega$ is of the form

$$y_1(x,t) = \sum_{n=1}^{\infty} Y_{1n}(x)q_{1n}(t). \tag{9}$$

Inserting Eq. (9) into Eq. (2) and reducing the resulting equation yields

$$\sum_{n=1}^{\infty} Y_{1n}\left(\ddot{q}_{1n} + p_n^2 q_{1n}\right) = -F\sin\omega t. \tag{10}$$

Introduce the orthogonality relationship between the mode shapes,

$$\int_0^l Y_{1n}Y_{1m}\,\mathrm{d}x = 0 \quad (n \neq m), \tag{11}$$

and Eq. (10) can be simplified into a set of uncoupled equations

$$\ddot{q}_{1n} + p_n^2 q_{1n} = C_n \sin \omega t \quad (n = 1, 2, ...), \tag{12}$$

where

$$C_n = -F \int_0^l Y_{1n} \, dx / \int_0^l Y_{1n}^2 \, dx. \tag{13}$$

The solution for Eq. (12) is

$$q_{1n} = \frac{C_n}{p_n^2 - \omega^2} \sin \omega t \quad (n = 1, 2, ...). \tag{14}$$

It is noted that Eq. (14) is valid when the shock frequency is not equal to the natural frequencies of the system. From Eq. (9) the response of the beam becomes

$$y_1(x, t) = \sum_{n=1}^{\infty} \frac{C_n Y_{1n}(x)}{p_n^2 - \omega^2} \sin \omega t \quad (0 \leqslant t \leqslant \pi/\omega), \tag{15}$$

which in turn leads to the vibration amplitude of the beam

$$\tilde{Y}_1(x) = \sum_{n=1}^{\infty} \frac{C_n Y_{1n}(x)}{p_n^2 - \omega^2}. \tag{16}$$

3. Linear dynamic analysis of the optical fibers

In this section, it is assumed that the tension in the string is constant. The time period $0 \leqslant t \leqslant \pi/\omega$ is no longer explicitly specified from now on, though all the vibration analysis is still limited in this period. The equation of motion for the string is obtained as

$$a^2 \frac{\partial^2 y_2}{\partial x^2} - \frac{\partial^2 y_2}{\partial t^2} = F \sin \omega t, \tag{17}$$

where

$$a = \sqrt{\frac{T_0}{\rho_2 A_2}}, \tag{18}$$

in which T_0, ρ_2, A_2 are the constant tension, the mass density and the cross section area of the string, respectively. The boundary conditions for Eq. (17) are

$$y_2(0, t) = y_1(0, t), y_2(L_0, t) = y_1(L_0, t), y_2(l - L_0, t) = y_1(l - L_0, t), y_2(l, t) = y_1(l, t), \tag{19}$$

in which $x = 0$, L_0, $l - L_0$, l indicate the positions where the string is bonded to the beam, as shown in Fig. 2. Clearly, the boundary conditions for the string are coupled with the response of the beam, which distinguishes this problem from other string or beam problems and adds to its complexity.

In order to uncouple the boundary conditions for the string from the beam response, introduce the following transformation which yields new variables indicating the relative deflection of the

string with respect to the beam:

$$z_{2i} = y_{2i} - y_1 \quad (i = 1, 2, 3), \tag{20}$$

where y_{21}, y_{22} and y_{23} denote the string deflection y_2 at position x in different ranges of $[0, L_0)$, $[L_0, l\text{-}L_0)$ and $[l\text{-}L_0, l]$, respectively. Replacing y_2 with the above variables in Eqs. (17) and (19) results in

$$a^2\frac{\partial^2 z_{2i}}{\partial x^2} - \frac{\partial^2 z_{2i}}{\partial t^2} = F \sin \omega t - \left(a^2\frac{\partial^2 y_1}{\partial x^2} - \frac{\partial^2 y_1}{\partial t^2}\right) \quad (i = 1, 2, 3) \tag{21}$$

with the new boundary conditions

$$z_{21}(0, t) = 0, \qquad z_{21}(L_0, t) = 0\,, \tag{22}$$

$$z_{22}(L_0, t) = 0, \qquad z_{22}(l - L_0, t) = 0\,, \tag{23}$$

$$z_{23}(l - L_0, t) = 0, \qquad z_{23}(l, t) = 0\,. \tag{24}$$

In what follows, each of the three sections of the string is treated separately. First, the natural frequencies and the mode shapes for the free vibration are obtained; then, assume the response to the forced vibration in a series form, and the response in analytical form is derived with the aid of the orthogonality relationship between the mode shapes.

Substituting Eq. (15) into Eq. (21) yields

$$a^2\frac{\partial^2 z_{2i}}{\partial x^2} - \frac{\partial^2 z_{2i}}{\partial t^2} = f(x, t) = \bar{f}(x)\sin \omega t \quad (i = 1, 2, 3). \tag{25}$$

where

$$\bar{f}(x) = F - a^2 \sum_{n=1}^{\infty} \frac{C_n}{p_n^2 - \omega^2} \frac{\mathrm{d}^2 Y_{1n}}{\mathrm{d}x^2} - \omega^2 \sum_{n=1}^{\infty} \frac{C_n Y_{1n}}{p_n^2 - \omega^2}. \tag{26}$$

For the following free vibration equation which corresponds to Eq. (25)

$$a^2\frac{\partial^2 z_{2i}}{\partial x^2} - \frac{\partial^2 z_{2i}}{\partial t^2} = 0 \quad (i = 1, 2, 3), \tag{27}$$

it is supposed that the solution takes the form

$$\bar{z}_{2i}(x, t) = \left(A_{2i}^* \sin \frac{p_{2i}^*}{a} x + B_{2i}^* \cos \frac{p_{2i}^*}{a} x\right) \sin\left(p_{2i}^* t + \varphi_{2i}^*\right) \quad (i = 1, 2, 3), \tag{28}$$

where A_{2i}^* and B_{2i}^* are undetermined constants, and p_{2i}^* and φ_{2i}^* are the natural frequency and the phase angle, respectively. Substituting Eq. (28) into the boundary conditions for the section of string lying in $[0, L_0]$, i.e., Eq. (22), gives

$$B_{21}^* = 0, \quad p_{21}^{*n} = \frac{na\pi}{L_0} \ (n = 1, 2, \ldots), \tag{29}$$

which, together with Eq. (28), leads to the mode shapes of the section of string lying in $[0, L_0]$

$$Z_{21}^n(x) = \sin\frac{n\pi}{L_0} x \quad (n = 1, 2, \ldots). \tag{30}$$

Similarly, the natural frequencies and the mode shapes of the sections of the string in $[L_0, l\text{-}L_0]$ and $[l\text{-}L_0, l]$ are obtained

$$p_{22}^{*n} = \frac{na\pi}{l-2L_0},$$
$$Z_{22}^n(x) = \sin\frac{n\pi}{l-2L_0}x - \tan\frac{n\pi L_0}{l-2L_0}\cos\frac{n\pi}{l-2L_0}x, \quad (n = 1, 2, ...), \tag{31}$$

$$p_{23}^{*n} = \frac{na\pi}{L_0},$$
$$Z_{23}^n(x) = \sin\frac{n\pi}{L_0}x - \tan\frac{n\pi l}{L_0}\cos\frac{n\pi}{L_0}x, \quad (n = 1, 2, ...). \tag{32}$$

Assuming that $z_{2i}(x, t)$ takes the form

$$z_{2i}(x,t) = \sum_{n=1}^{\infty} Z_{2i}^n(x) q_{2i}^n(t) \quad (i = 1, 2, 3) \tag{33}$$

and substituting it into Eq. (25), it is derived that

$$\sum_{n=1}^{\infty} Z_{2i}^n\left(\ddot{q}_{2i}^n + p_{2i}^{*n2} q_{2i}^n\right) = -f(x,t) \quad (i = 1, 2, 3). \tag{34}$$

Applying the orthogonality relationship between the mode shapes,

$$\int_{\bar{l}} Z_{2i}^n Z_{2i}^m \, \mathrm{d}x = 0 \ \ (n \neq m) \ \ (i = 1, 2, 3), \tag{35}$$

where $\bar{l}$ denotes the integration domain, Eq. (34) can be reduced to a set of uncoupled equations

$$\ddot{q}_{2i}^n + p_{2i}^{*n2} q_{2i}^n = C_{2i}^n \sin\omega t \quad (i = 1, 2, 3; n = 1, 2, ...), \tag{36}$$

where

$$C_{21}^n = -\int_0^{L_0} \bar{f}(x) Z_{21}^n(x) \, \mathrm{d}x \Big/ \int_0^{L_0} Z_{21}^{n2}(x) \, \mathrm{d}x,$$
$$C_{22}^n = -\int_{L_0}^{l-L_0} \bar{f}(x) Z_{22}^n(x) \, \mathrm{d}x \Big/ \int_{L_0}^{l-L_0} Z_{22}^{n2}(x) \, \mathrm{d}x,$$
$$C_{23}^n = -\int_{l-L_0}^{l} \bar{f}(x) Z_{23}^n(x) \, \mathrm{d}x \Big/ \int_{l-L_0}^{l} Z_{23}^{n2}(x) \, \mathrm{d}x. \tag{37}$$

Obviously, from Eq. (36) we have

$$q_{2i}^n(t) = \frac{C_{2i}^n}{p_{2i}^{*n2} - \omega^2} \sin\omega t \quad (i = 1, 2, 3; \ \ n = 1, 2, ...). \tag{38}$$

Making use of Eqs. (20), (30)–(33) and (38), the deflection of the string can be obtained:

$$y_{21}(x,t)=\sum_{n=1}^{\infty}\sin\frac{n\pi}{L_0}x\cdot\frac{C_{21}^n}{p_{21}^{*n2}-\omega^2}\sin\,\omega t+y_1(x,t),$$

$$y_{22}(x,t)=\sum_{n=1}^{\infty}\left(\sin\frac{n\pi}{l-2L_0}x-\tan\frac{n\pi L_0}{l-2L_0}\cos\frac{n\pi}{l-2L_0}x\right)\frac{C_{22}^n}{p_{22}^{*n2}-\omega^2}\sin\,\omega t+y_1(x,t),$$

$$y_{23}(x,t)=\sum_{n=1}^{\infty}\left(\sin\frac{n\pi}{L_0}x-\tan\frac{n\pi l}{L_0}\cos\frac{n\pi}{L_0}x\right)\frac{C_{23}^n}{p_{23}^{*n2}-\omega^2}\sin\,\omega t+y_1(x,t), \tag{39}$$

where $y_1(x,\,t)$ is the deflection of the beam as in Eq. (15). Finally, the vibration amplitude of the string is derived from Eq. (39):

$$\tilde{Y}_2(x)=\begin{cases}\sum_{n=1}^{\infty}\left[\sin\dfrac{n\pi}{L_0}x\cdot\dfrac{C_{21}^n}{p_{21}^{*n2}-\omega^2}+Y_{1n}(x)\dfrac{C_n}{p_n^2-\omega^2}\right], & x\in[0,L_0],\\ \sum_{n=1}^{\infty}\left[\left(\sin\dfrac{n\pi}{l-2L_0}x-\tan\dfrac{n\pi L_0}{l-2L_0}\cos\dfrac{n\pi}{l-2L_0}x\right)\dfrac{C_{22}^n}{p_{22}^{*n2}-\omega^2}+Y_{1n}(x)\dfrac{C_n}{p_n^2-\omega^2}\right], & x\in[L_0,l-L_0],\\ \sum_{n=1}^{\infty}\left[\left(\sin\dfrac{n\pi}{L_0}x-\tan\dfrac{n\pi l}{L_0}\cos\dfrac{n\pi}{L_0}x\right)\dfrac{C_{23}^n}{p_{23}^{*n2}-\omega^2}+Y_{1n}(x)\dfrac{C_n}{p_n^2-\omega^2}\right], & x\in[l-L_0,l].\end{cases} \tag{40}$$

4. Non-linear dynamic analysis of the optical fibers

In this section, geometrical non-linearity is incorporated in the modelling to describe large transverse vibration of the string. The tension in the string varies with deflection and thereby is a function of time. It is assumed, however, that the tension does not vary with position, namely, it is a constant with respect to different positions. It is also noted that the symbols defined in the previous section keep the same here.

For the string, the total length is now a function of time t:

$$\bar{l}(t)=\int_0^l\sqrt{1+\left(\frac{\partial y_2}{\partial x}\right)^2}\,\mathrm{d}x, \tag{41}$$

and the tension in the string becomes

$$T=T_0+K_s(\bar{l}-l), \tag{42}$$

where T_0 is the initial tension and K_s is the elastic coefficient of the string. The governing equation of motion for the string is obtained as

$$\left[K_s\int_0^l\sqrt{1+\left(\frac{\partial y_2}{\partial x}\right)^2}\,\mathrm{d}x+T_0-K_sl\right]\frac{\partial^2y_2}{\partial x^2}-\rho_2A_2\frac{\partial^2y_2}{\partial t^2}=\rho_2A_2F\sin\,\omega t \tag{43}$$

whose boundary conditions remain the same:

$$\begin{aligned} y_2(0,t) &= y_1(0,t),\\ y_2(L_0,t) &= y_1(L_0,t),\\ y_2(l-L_0,t) &= y_1(l-L_0,t),\\ y_2(l,t) &= y_1(l,t). \end{aligned} \tag{44}$$

With the approximation

$$\sqrt{1+\left(\frac{\partial y_2}{\partial x}\right)^2} \approx 1+\frac{1}{2}\left(\frac{\partial y_2}{\partial x}\right)^2, \tag{45}$$

Eq. (43) can be expressed as

$$\left[\frac{1}{2}K_s\int_0^l\left(\frac{\partial y_2}{\partial x}\right)^2 \mathrm{d}x + T_0\right]\frac{\partial^2 y_2}{\partial x^2} - \rho_2 A_2\frac{\partial^2 y_2}{\partial t^2} = \rho_2 A_2 F\sin\omega t. \tag{46}$$

It is easily seen that the above equation is a non-linear one, which makes the problem more complex. As in the last section, the following transformation is introduced to solve the coupling in the boundary conditions for the string, Eq. (44):

$$z_{2i} = y_{2i} - y_1 \quad (i=1,2,3). \tag{47}$$

Substituting Eq. (47) into Eq. (46) yields

$$\begin{aligned} &\left\{T_0+\frac{1}{2}K_s\left[\int_0^{L_0}\left(\frac{\partial z_{21}}{\partial x}+\frac{\partial y_1}{\partial x}\right).^2\,\mathrm{d}x + \int_{L_0}^{l-L_0}\left(\frac{\partial z_{22}}{\partial x}+\frac{\partial y_1}{\partial x}\right)^2\mathrm{d}x\right.\right.\\ &\left.\left.+\int_{l-L_0}^{l}\left(\frac{\partial z_{23}}{\partial x}+\frac{\partial y_1}{\partial x}\right)^2\mathrm{d}x\right]\right\}\left(\frac{\partial^2 z_{2i}}{\partial x^2}+\frac{\partial^2 y_1}{\partial x^2}\right) - \rho_2 A_2\left(\frac{\partial^2 z_{2i}}{\partial t^2}+\frac{\partial^2 y_1}{\partial t^2}\right) = \rho_2 A_2 F\sin\omega t,\ (i=1,2,3), \end{aligned} \tag{48}$$

with the boundary conditions

$$z_{21}(0,t)=0, \qquad z_{21}(L_0,t)=0, \tag{49}$$

$$z_{22}(L_0,t)=0, \qquad z_{22}(l-L_0,t)=0, \tag{50}$$

$$z_{23}(l-L_0,t)=0, \qquad z_{23}(l,t)=0. \tag{51}$$

In the following discussion, a similar approach is taken to solve the vibration response of the string, namely, three sections of the string are dealt with separately. The response solution is supposed to take a series form satisfying the boundary conditions, and the differential equations are simplified into a set of uncoupled equations. However, the final solution can not be reached in analytical form due to the complexity caused by the non-linear factor.

Suppose

$$z_{2i}(x,t) = \sum_{n=1}^{\infty} C_{in}(x)q_{in}(t) \quad (i=1,2,3), \tag{52}$$

where

$$C_{1n}(x) = \sin\frac{n\pi x}{L_0}, \tag{53}$$

$$C_{2n}(x) = \sin\frac{n\pi x}{l-2L_0} - \tan\frac{n\pi L_0}{l-2L_0}\ \cos\frac{n\pi x}{l-2L_0}, \tag{54}$$

$$C_{3n}(x) = \sin\frac{n\pi x}{L_0} - \tan\frac{n\pi l}{L_0}\ \cos\frac{n\pi x}{L_0}. \tag{55}$$

It can be easily seen that Eq. (52) satisfies the boundary conditions, Eqs. (49)–(51). Inserting Eq. (52) into Eq. (48) gives

$$\begin{aligned}&\left\{T_0 + \frac{1}{2}K_s\left[\int_0^{L_0}\left(\sum_{n=1}^{\infty} C'_{1n}(x)q_{1n} + \tilde{Y}'_1(x)\sin\omega t\right)^2 \mathrm{d}x + \int_{L_0}^{l-L_0}\left(\sum_{n=1}^{\infty} C'_{2n}(x)q_{2n} + \tilde{Y}'_1(x)\sin\omega t\right)^2 \mathrm{d}x\right.\right.\\ &\left.\left.+\int_{l-L_0}^{l}\left(\sum_{n=1}^{\infty} C'_{3n}(x)q_{3n} + \tilde{Y}'_1(x)\sin\,\omega t\right)^2 \mathrm{d}x\right]\right\}\cdot\left(\sum_{n=1}^{\infty} C''_{in}(x)q_{in} + \tilde{Y}''_1(x)\sin\,\omega t\right)\\ &-\rho_2 A_2\left[\sum_{n=1}^{\infty} C_{in}(x)\ddot{q}_{in} - \omega^2\,\tilde{Y}_1(x)\sin\,\omega t\right] = \rho_2 A_2 F\,\sin\,\omega t, \quad (i=1,2,3),\end{aligned} \tag{56}$$

where

$$C'_{1n}(x) = \frac{n\pi}{L_0}\cos\frac{n\pi x}{L_0}, \tag{57}$$

$$C'_{2n}(x) = \frac{n\pi}{l-2L_0}\left(\cos\frac{n\pi x}{l-2L_0} + \tan\frac{n\pi L_0}{l-2L_0}\sin\frac{n\pi x}{l-2L_0}\right), \tag{58}$$

$$C'_{3n}(x) = \frac{n\pi}{L_0}\left(\cos\frac{n\pi x}{L_0} + \tan\frac{n\pi l}{L_0}\sin\frac{n\pi x}{L_0}\right), \tag{59}$$

$$\tilde{Y}'_1(x) = \sum_{n=1}^{\infty}\frac{C_n K^*}{p_n^2-\omega^2}\left[K_A\cos\,K^*x - \sin\,K^*x + K_C\cosh\,K^*x + \sinh\,K^*x\right] \tag{60}$$

in which K^* is the same as in Eq. (5) and K_A, K_C the same as in Eq. (7). By using the following definition

$$\begin{aligned}K_{coe}(q_{1n},q_{2n},q_{3n},t) &= \int_0^{L_0}\left(\sum_{n=1}^{\infty} C'_{1n}(x)q_{1n} + \tilde{Y}'_1(x)\sin\omega t\right)^2 \mathrm{d}x\\ &+\int_{L_0}^{l-L_0}\left(\sum_{n=1}^{\infty} C'_{2n}(x)q_{2n} + \tilde{Y}'_1(x)\sin\omega t\right)^2 \mathrm{d}x + \int_{l-L_0}^{l}\left(\sum_{n=1}^{\infty} C'_{3n}(x)q_{3n} + \tilde{Y}'_1(x)\sin\omega t\right)^2 \mathrm{d}x,\end{aligned} \tag{61}$$

$$T_{0^*} = T_0/\rho_2 A_2, \qquad K_{s^*} = K_s/\rho_2 A_2, \tag{62, 63}$$

Eq. (56) can take a simpler form

$$\begin{aligned}&\left(T_{0^*} + \frac{1}{2}K_{coe}K_{s^*}\right)\cdot\left(\sum_{n=1}^{\infty} C''_{in}(x)q_{in} + \tilde{Y}''_1(x)\sin\omega t\right) - \sum_{n=1}^{\infty} C_{in}(x)\ddot{q}_{in}\\ &+\omega^2\,\tilde{Y}_1(x)\sin\omega t = F\,\sin\,\omega t \quad (i=1,2,3).\end{aligned} \tag{64}$$

Multiplying Eq. (64) by $C_{in}(x)$ ($i=1,2,3$; $n=1,2,\ldots$) and performing the integration results in a group of equations where the time derivative terms $\ddot{q}_{in}(i=1,2,3; n=1,2,\cdots)$ are uncoupled:

$$\left(T_{0*}+\frac{1}{2}K_{s*}K_{coe}\right)\left[\sum_{m=1}^{\infty}\left(\int_0^{L_0} C''_{1m}(x)C_{1n}(x)\,\mathrm{d}x\right)q_{1m}+\int_0^{L_0}\tilde{Y}''_1(x)C_{1n}(x)\,\mathrm{d}x\sin\omega t\right]$$
$$-\int_0^{L_0} C^2_{1n}(x)\,\mathrm{d}x\ddot{q}_{1n}+\omega^2\int_0^{L_0}\tilde{Y}_1(x)C_{1n}(x)\,\mathrm{d}x\sin\omega t=\int_0^{L_0} C_{1n}(x)\,\mathrm{d}xF\sin\omega t\quad(n=1,2,\cdots), \tag{65}$$

$$\left(T_{0*}+\frac{1}{2}K_{s*}K_{coe}\right)\left[\sum_{m=1}^{\infty}\left(\int_{L_0}^{l-L_0} C''_{2m}(x)C_{2n}(x)\,\mathrm{d}x\right)q_{2m}+\int_{L_0}^{l-L_0}\tilde{Y}''_1(x)C_{2n}(x)\,\mathrm{d}x\sin\omega t\right]$$
$$-\int_{L_0}^{l-L_0} C^2_{2n}(x)\,\mathrm{d}x\ddot{q}_{2n}+\omega^2\int_{L_0}^{l-L_0}\tilde{Y}_1(x)C_{2n}(x)\,\mathrm{d}x\sin\omega t=\int_{L_0}^{l-L_0} C_{2n}(x)\,\mathrm{d}xF\sin\omega t\quad(n=1,2,\cdots), \tag{66}$$

$$\left(T_{0*}+\frac{1}{2}K_{s*}K_{coe}\right)\left[\sum_{m=1}^{\infty}\left(\int_{l-L_0}^{l} C''_{3m}(x)C_{3n}(x)\,\mathrm{d}x\right)q_{3m}+\int_{l-L_0}^{l}\tilde{Y}''_1(x)C_{3n}(x)\,\mathrm{d}x\sin\omega t\right]$$
$$-\int_{l-L_0}^{l} C^2_{3n}(x)\,\mathrm{d}x\ddot{q}_{3n}+\omega^2\int_{l-L_0}^{l}\tilde{Y}_1(x)C_{3n}(x)\,\mathrm{d}x\sin\omega t=\int_{l-L_0}^{l} C_{3n}(x)\,dxF\sin\omega t\quad(n=1,2,\cdots). \tag{67}$$

Employing numerical methods, q_{1n}, q_{2n} and q_{3n} ($n=1,2,\ldots,n_{max}$) can be solved from the above equations with a given n_{max}, where n_{max} is the highest order of the modal functions used in evaluating the vibration response and is chosen on the basis of the precision requirement of the response. With q_{1n}, q_{2n} and q_{3n} ($n=1,2,\ldots,n_{max}$) solved, z_{2i} and y_{2i} ($i=1,2,3$) can be obtained from Eqs. (52) and (47), respectively.

5. Numerical results

For both linear and non-linear models, numerical simulations are performed to study the vibration of an optical fiber coupler subject to a 1000 g, 0.5 ms half sine shock motion. The basic system parameters used are given in Table 1, while K, L_0, T_0 and K_s are chosen as parameters for study, whose scope of values is provided in Table 2. Table 3 shows the default values of these parameters—since only one parameter is studied at a time, the other parameters are assumed to take the default values. The parameter values used for numerical simulations are set according to physical properties of real substrates and fibers.

For the linear model, the numerical results are shown in Figs. 3–5, where curves of the vibration amplitude of the string and the beam versus the position are drawn. It should be mentioned that in these figures the beam deflection is actually curved, although it looks like a straight line due to the very small deflection. It is noted that in the following analysis, the vibration amplitudes of the string for different values of a parameter are compared on the basis of the middle span. In Fig. 3,

Table 1
System parameters

The length of the beam l	0.04 m
The area of cross section of the beam A_1	$6.61 \times 10^{-6}\,m^2$
The mass density of the beam ρ_1	$2200\,kg/m^3$
Young's modulus of the beam E	$7.24 \times 10^{10}\,Pa$
The moment of inertia of the beam cross-section J	$4.34 \times 10^{-12}\,m^4$
The area of cross-section of the string A_2	$3.1 \times 10^{-8}\,m^2$
The mass density of the string ρ_2	$2200\,kg/m^3$
The acceleration of the shock motion F	$9800\,m/s^2$
The circular frequency of the shock motion ω	$2\pi \times 10^3\,rad/s$

Table 2
Parameter range for parametric study

The string (initial) tension T_0	0.01–0.60 N
The spring stiffness K	1000–40000 N/m
The position of bonding points L_0	0.005–0.0175 m
The elastic coefficient of the string K_s	0–20000 N/m

Table 3
Default parameter values

The string (initial) tension T_0	0.06 N
The spring stiffness K	5000 N/m
The position of bonding points L_0	0.01 m
The elastic coefficient of the string K_s	5000 N/m

the spring stiffness K is taken as a parameter which ranges from 1000 to 40000 N/m. It is shown that the vibration of the string is the largest at $K = 10000$ N/m and decreases as K increases or decreases further. It is also found that for K equal to 1000 N/m, the vibration of the string is the smallest. Interestingly, the beam amplitude increases as the spring stiffness K increases for relatively small K values (1000–10000 N/m), and the effect is just opposite for relatively large K values (10000–40000 N/m).

Fig. 4 shows the vibration amplitude as a function of the position for various locations of bonding points. It is seen that the vibration is largest when the bonding points are most evenly distributed along the span. It is also shown that when the bonding points are farthest from the ends of the span, the vibration of the string becomes the smallest.

In Fig. 5, with the initial tension T_0 from 0.02 to 0.60 N selected as the parameter, no clear change tendency of the vibration amplitude along with the parameter T_0 appears. It is only shown that the vibration of the string is the largest when the initial tension is at 0.1 N and is the smallest

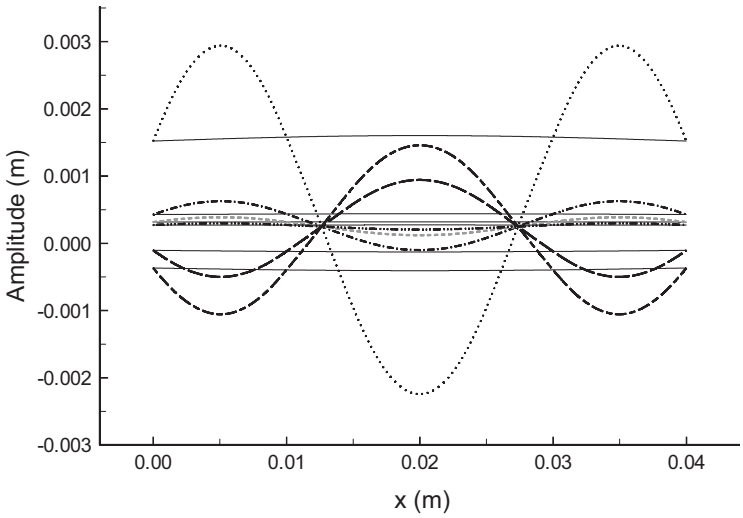

Fig. 3. Amplitude response of the string and the beam with spring stiffness as parameter in linear model analysis: ——, beam; ....., $K = 10\,000$ N/m; _._._._, $K = 5000$ N/m; - - - - -, $K = 2500$ N/m; _.._.._.._, $K = 1000$ N/m; — — —, $K = 40\,000$ N/m; - - -, $K = 20\,000$ N/m.

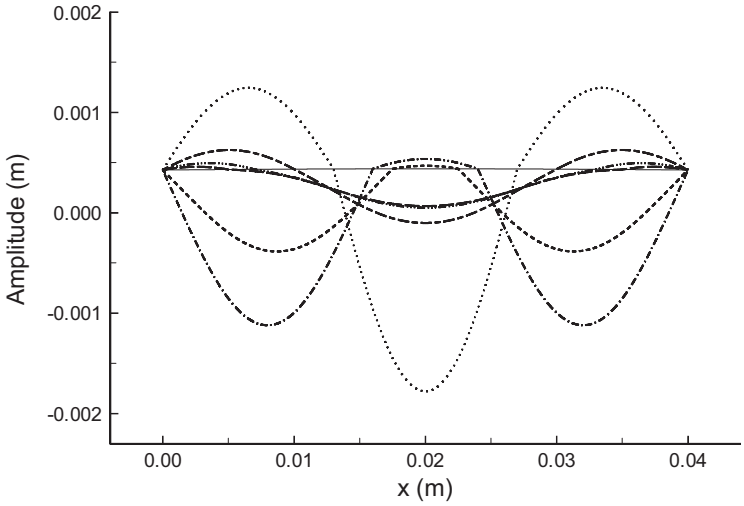

Fig. 4. Amplitude response of the string and the beam with bonding location as parameter in linear model analysis: ——, beam; ....., $L_0 = 13$ mm; _._._._, $L_0 = 16$ mm; - - - - -, $L_0 = 17.5$ mm; _.._.._.._, $L_0 = 7$ mm; — — —, $L_0 = 5$ mm; - - -, $L_0 = 10$ mm.

when the initial tension is at 0.6 N. However, if we divide the initial tensions into two groups, i.e., {0.40 N, 0.60 N} and {0.02 N, 0.06 N, 0.10 N}, it is seen that the group of larger initial tensions corresponds to smaller string amplitude, which is physically reasonable. Furthermore, this tendency holds for the relatively large parameter values, namely, 0.40 N and 0.60 N.

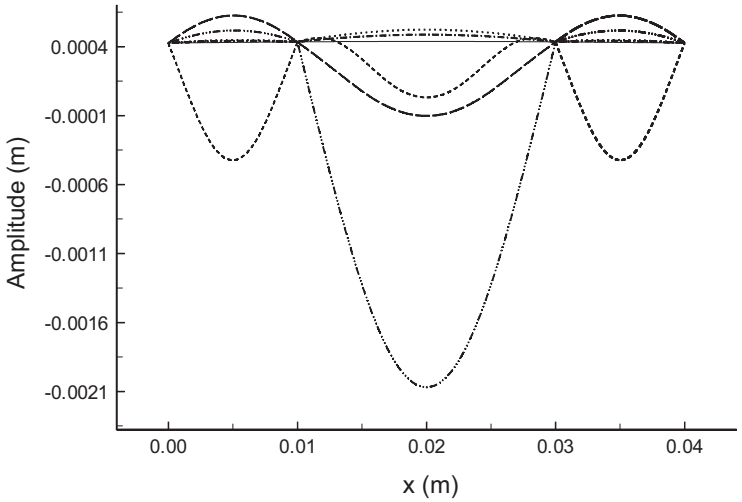

Fig. 5. Amplitude response of the string and the beam with initial tension as parameter in linear model analysis: ——, beam; ....., $T_0 = 0.40$ N; ._._._._, $T_0 = 0.60$ N; - - - - -, $T_0 = 0.02$ N; ._...._..., $T_0 = 0.10$ N; — — —, $T_0 = 0.06$ N.

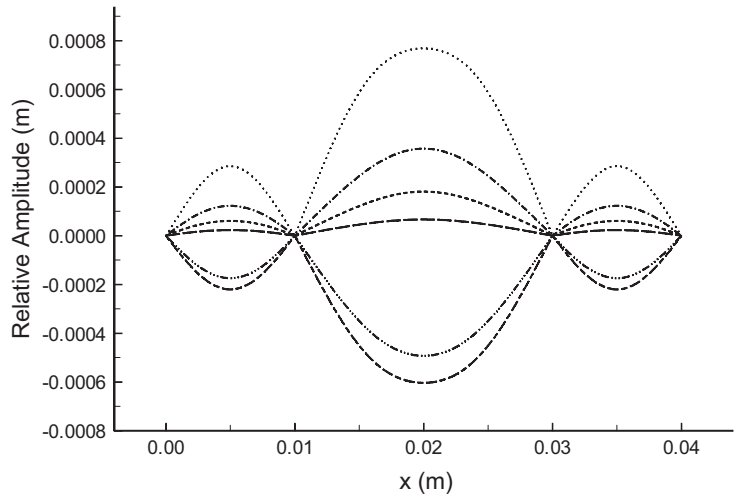

Fig. 6. Relative amplitude response of the string with spring stiffness as parameter in non-linear model analysis: ....., $K = 10\,000$ N/m; ._._._._, $K = 5000$ N/m; - - - - -, $K = 2500$ N/m; ._...._..., $K = 40\,000$ N/m; — — —, $K = 1000$ N/m; - - - -, $K = 20\,000$ N/m.

For the non-linear model, the simulation results are shown in Figs. 6–9, in which curves of the relative vibration amplitude of the string with respect to the beam versus the position are plotted. In Fig. 6, the support stiffness K is chosen as a parameter whose value lies between 1000 and 40 000 N/m. It is obvious that the vibration of the string is the largest at $K = 10\,000$N/m and decreases as K increases or decreases from that value. This trend agrees with that predicted by the linear model. It is also shown that for $K = 1000$ N/m, the vibration of the string is the smallest.

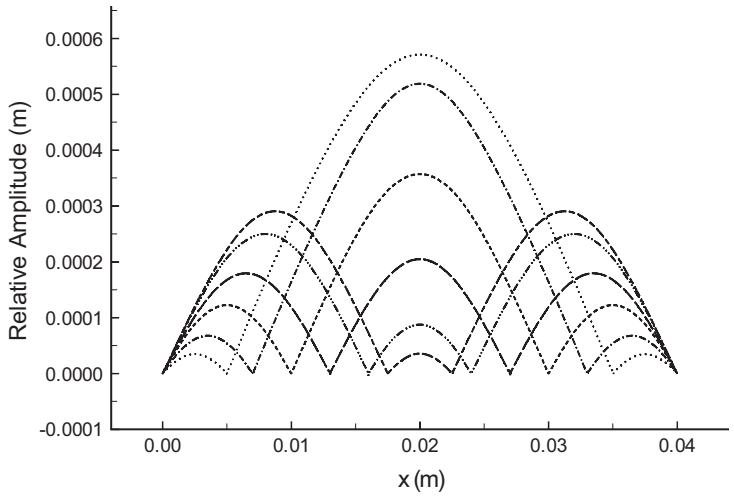

Fig. 7. Relative amplitude response of the string with bonding location as parameter in non-linear model analysis: ....., $L_0 = 5$ mm; _._._., $L_0 = 7$ mm; - - - - -, $L_0 = 10$ mm; _.._.._.., $L_0 = 16$ mm; — — —, $L_0 = 13$ mm; - - -, $L_0 = 17.5$ mm.

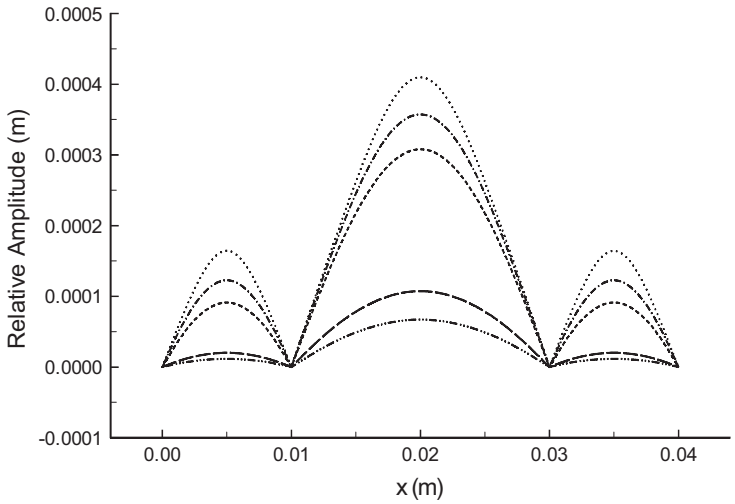

Fig. 8. Relative amplitude response of the string with initial tension as parameter in non-linear model analysis: ....., $T_0 = 0.02$ N; _._._., $T_0 = 0.06$ N; - - - - -, $T_0 = 0.10$ N; _.._.._.., $T_0 = 0.60$ N; — — —, $T_0 = 0.40$ N.

In Fig. 7, the curves of the relative vibration amplitude of the string versus the position are plotted for various locations of bonding points. It is seen that the closer the two middle bonding points are from the ends of the span, the larger the vibration is. This is expected since it is physically reasonable. The result is different from that from the linear model.

Fig. 8 shows the situation when the initial tension T_0 is a parameter ranging from 0.02 to 0.60 N. It is found that the larger the initial tension, the smaller the vibration of the string, which makes sense since larger initial tension makes the string stiffer and thus reduces the vibration. In

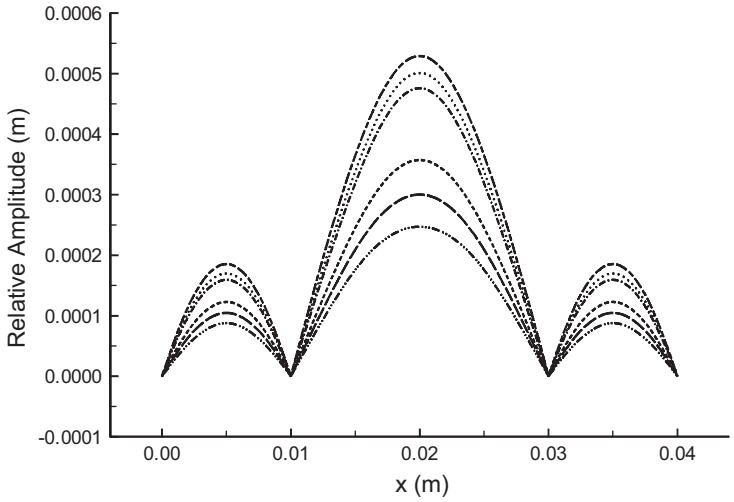

Fig. 9. Relative amplitude response of the string with elastic coefficient of the string as parameter in non-linear model analysis: ....., $K_s = 500$ N/m; ._._._., $K_s = 1000$ N/m; - - - - -, $K_s = 5000$ N/m; _.._.._.., $K_s = 20\,000$ N/m; — — —, $K_s = 10\,000$ N/m; - – - –, $K_s = 0$ N/m.

contrast, this physically reasonable tendency holds only for some (but not all) parameter values in the linear model simulations. This shows that the linear model is not adequate to describe the vibration of the optical fibers.

From Fig. 9, where the relative vibration amplitude of the string is plotted against the position with the elastic coefficient of the string K_s as a parameter which varies from 0 to 20 000 N/m, it is seen that as the string gets stiffer with larger K_s, the vibration gets smaller. This is right as stiffer strings will vibrate less.

6. Conclusions

In this paper, the vibration of an optical fiber coupler subject to a half sine shock is studied analytically and numerically, with emphasis laid on the dynamic behavior of the optical fibers inside the coupler and the influence of various coupler parameters upon the vibration of the optical fibers. Both linear and non-linear models are developed for the optical fibers. The non-linear model is a big improvement over the linear model, since the results predicted by this non-linear model are physically sound while the linear model predicts some physically unreasonable phenomena. Finally, the following conclusions are drawn from this paper and they provide some guidelines for the design of optical fiber couplers.

1. With support stiffness as a parameter, the vibration amplitude of the optical fibers reaches the largest at certain parameter value and decreases as the parameter increases or decreases further. Such parameter value should be avoided in designing optical fiber couplers.

2. The distribution of the bonding points has an influence on the vibration of the optical fibers, which means the closer the two middle bonding points are towards the ends of the span, the larger the vibration becomes. In the design, therefore, the middle bonding positions should be chosen not close to the ends of the substrate.
3. It is found that the larger the initial tension in the optical fibers, the smaller their vibration. So, reasonably large initial tension in optical fibers is recommended for the design of optical fiber couplers.
4. It is also shown that as the elastic coefficient of the optical fibers gets larger, the vibration gets smaller. Therefore, material with large elastic coefficient is ideal to make optical fibers in couplers, from a mechanics point of view.

References

[1] H.F. Wolf, Handbook of Fiber Optics: theory and applications, Garland STPM Press, New York, 1979.
[2] B.S. Kawasaki, Low-loss access coupler for multimode optical fiber distribution networks, Applied Optics 16 (1977) 1794–1795.
[3] J.C. Palais, Fiber Optic Communications, Prentice-Hall, Englewood Cliffs, NJ, 1988.
[4] G.V. Anand, Non-linear resonance in stretched strings with viscous damping, The Journal of Acoustical Society of America 40 (1966) 1517–1528.
[5] H.P.W. Gottlieb, Non-linear vibration of a constant-tension string, Journal of Sound and Vibration 143 (1990) 455–460.
[6] Z. Oniszczuk, Transverse vibrations of elastically connected double-string complex system, Part I: free vibrations, Journal of Sound and Vibration 232 (2000) 355–366.
[7] Z. Oniszczuk, Transverse vibrations of elastically connected double-string complex system, Part II: forced vibrations, Journal of Sound and Vibration 232 (2000) 367–386.
[8] M.U. Jen, E.B. Magrab, Natural frequencies and mode shapes of a beam carrying a two-degree-of-freedom–spring-mass system, Journal of Vibration and Acoustics 115 (1993) 202–209.
[9] M. Gurgoze, On the eigenfrequencies of a cantilever beam with attached tip mass and a spring–mass system, Journal of Sound and Vibration 190 (1996) 149–162.
[10] J.S. Wu, C.G. Huang, Free and forced vibration of a Timoshenko beam with any number of transactional and rotational springs and lumped masses, Communications in Numerical Methods in Engineering 11 (1995) 743–756.
[11] J.S. Wu, R.L. Lin, Free vibration analysis of a uniform cantilever beam with point masses by an analytical-and-numerical combined method, Journal of Sound and Vibration 136 (1990) 201–213.